

UHP-SOT: An Unsupervised High-Performance Single Object Tracker

Zhiruo Zhou¹, Hongyu Fu¹, Suya You², Christoph C. Borel-Donohue² and C.-C. Jay Kuo¹

¹ Media Communications Lab, University of Southern California, Los Angeles, CA, USA

² Army Research Laboratory, Adelphi, Maryland, USA

Abstract—An unsupervised online object tracking method that exploits both foreground and background correlations is proposed and named UHP-SOT (Unsupervised High-Performance Single Object Tracker) in this work. UHP-SOT consists of three modules: 1) appearance model update, 2) background motion modeling, and 3) trajectory-based box prediction. A state-of-the-art discriminative correlation filters (DCF) based tracker is adopted by UHP-SOT as the first module. We point out shortcomings of using the first module alone such as failure in recovering from tracking loss and inflexibility in object box adaptation and then propose the second and third modules to overcome them. Both are novel in single object tracking (SOT). We test UHP-SOT on two popular object tracking benchmarks, TB-50 and TB-100, and show that it outperforms all previous unsupervised SOT methods, achieves a performance comparable with the best supervised deep-learning-based SOT methods, and operates at a fast speed (i.e. 22.7-32.0 FPS on a CPU).

Index Terms—object tracking, online tracking, single object tracking, unsupervised tracking

I. INTRODUCTION

Video object tracking is one of the fundamental computer vision problems and has found rich applications in video surveillance [1], autonomous navigation [2], robotics vision [3], etc. In the setting of online single object tracking (SOT), a tracker is given a bounding box on the target object at the first frame and then predicts its boxes for all remaining frames [4]. Online tracking methods can be categorized into two categories, unsupervised and supervised [5]. Traditional trackers are unsupervised. Recent deep-learning-based (DL-based) trackers demand supervision. Unsupervised trackers are attractive since they do not need annotated boxes to train supervised trackers. The performance of trackers can be measured in terms of accuracy (higher success rate), robustness (automatic recovery from tracking loss), and speed (higher FPS).

We examine the design of an unsupervised high-performance tracker and name it UHP-SOT (Unsupervised High-Performance Single Object Tracker) in this work. UHP-SOT consists of three modules: 1) appearance model update, 2) background motion modeling, and 3) trajectory-based box prediction. Previous unsupervised trackers pay attention to efficient and effective appearance model update. Built upon this foundation, an unsupervised discriminative-correlation-filters-based (DCF-based) tracker is adopted by UHP-SOT as the baseline in the first module. Yet, the use of the first module alone has shortcomings such as failure in tracking loss recovery and being weak in box size adaptation. We propose ideas for background motion modeling and trajectory-based box prediction. Both are novel in SOT. We test UHP-SOT on two popular object tracking benchmarks, TB-50 and TB-100 [6], and show that it outperforms all previous unsupervised SOT methods, achieves a performance comparable with the best supervised DL-based SOT methods, and operates at a fast speed (22.7-32.0 FPS on a CPU).

II. RELATED WORK

DCF-based trackers. DCF-based trackers provide an efficient unsupervised SOT solution with quite a few variants, e.g., [7]–[14].

Generally speaking, they conduct dense sampling around the object patch and solve a rigid regression problem to learn a template for similarity matching. Under the periodic assumption of dense samples, they learn the template efficiently in the Fourier domain and achieve a fast tracking speed. Spatial-temporal regularized correlation filters (STRCF) [12] adds spatial-temporal regularization to the template learning process and performs favorably against other methods [15]–[18].

DL-based trackers. DL-based trackers offer a supervised SOT solution. Some of them use a pre-trained network [19], [20] as a feature extractor and do online tracking based on extracted deep features [10], [16], [21]–[23]. Others adopt an end-to-end model that is either trained by offline video datasets [15], [24] or adapted to the online video frames [25]–[28]. Recently, Siamese trackers [15], [24], [29]–[33] are gaining attention due to the simplicity and effectiveness. They treat the tracking as a problem of template matching in a large search region. Unsupervised training in large-scale offline datasets was investigated in [34] and [35].

III. PROPOSED UHP-SOT METHOD

System Overview. There are three main challenges in SOT:

- 1) significant change of object appearance,
- 2) loss of tracking,
- 3) rapid variation of object's location and/or shape.

To address these challenges, we propose a new tracker, UHP-SOT, whose system diagram is shown in Fig. 1. As shown in the figure, it consists of three modules:

- 1) appearance model update,
- 2) background motion modeling,
- 3) trajectory-based box prediction.

UHP-SOT follows the classic tracking-by-detection paradigm where the object is detected within a region centered at its last predicted location at each frame. The histogram of gradients (HOG) and color name (CN) [36] features are extracted to yield the feature map. We choose the STRCF tracker [12] as the baseline tracker. However, STRCF cannot handle the second and the third challenges well, as shown in Fig. 2. We propose the second and the third modules in UHP-SOT to address them. They are the main contributions of this work. UHP-SOT operates in the following fashion. The baseline tracker gets initialized at the first frame. For the following frames, UHP-SOT gets proposals from all three modules and chooses one of them as the final prediction based on a fusion strategy. They are elaborated below.

Spatial-temporal regularized correlation filters (STRCF). In STRCF, the object appearance at frame t is modeled by a template denoted by \mathbf{f}_t . It is used for similarity matching at frame $(t + 1)$. The template is initialized at the first frame. Assume that the cropped patch centered at the object location has a size of $N_x \times N_y$ pixels at

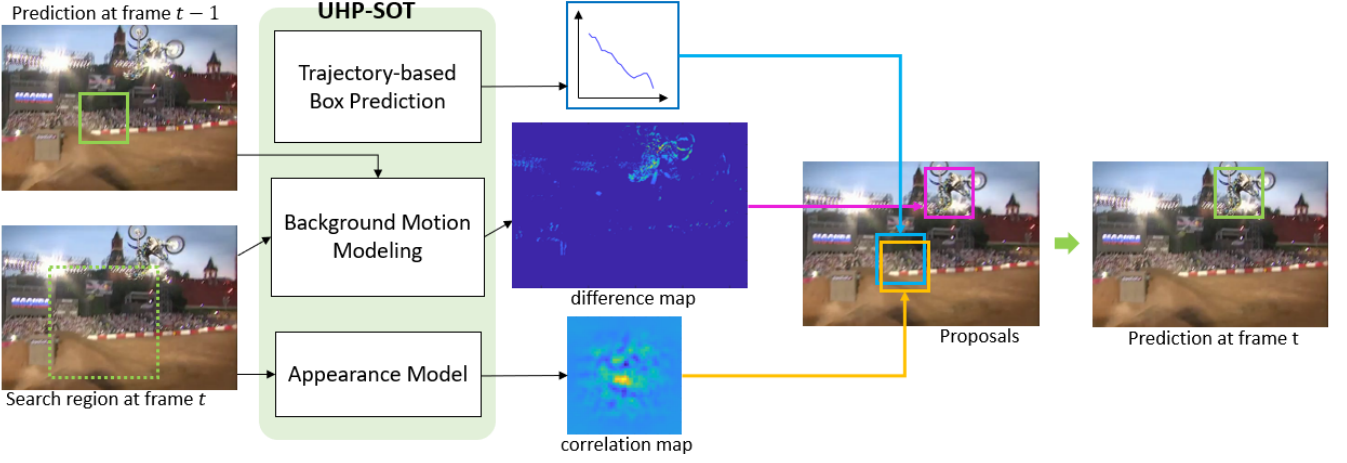


Fig. 1. The system diagram of the proposed UHP-SOT method. In the example, the object was lost at time $t - 1$ but gets retrieved at time t because the proposal from background motion modeling is accepted.

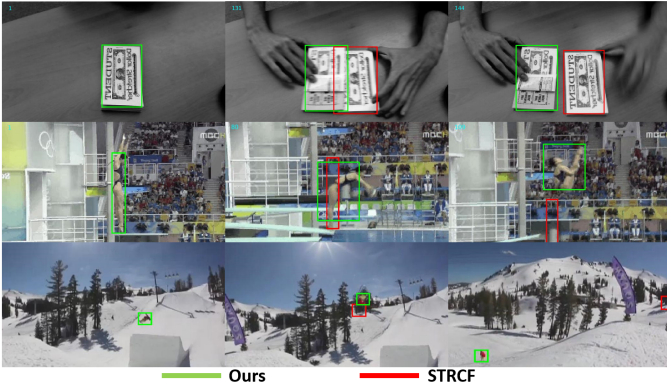


Fig. 2. Comparison of the tracking performance of STRCF (red) and UHP-SOT (green), where the results of UHP-SOT are closer to the ground truth and those of STRCF drift away.

frame t . Then, the template gets updated at frame t by solving the following regression equation:

$$\arg \min_{\mathbf{f}} \frac{1}{2} \left\| \sum_{d=1}^D \mathbf{x}_t^d * \mathbf{f}^d - \mathbf{y} \right\|^2 + \frac{1}{2} \sum_{d=1}^D \left\| \mathbf{w} \cdot \mathbf{f}^d \right\|^2 + \frac{\mu}{2} \left\| \mathbf{f} - \mathbf{f}_{t-1} \right\|^2,$$

where $\mathbf{y} \in \mathbb{R}^{N_x \times N_y}$ is a centered Gaussian-shaped map used as regression labels, $\mathbf{x}_t \in \mathbb{R}^{N_x \times N_y \times D}$ is the spatial map of D features, $*$ denotes the spatial convolution of the same feature, \mathbf{w} is the spatial weight on the template, \mathbf{f}_{t-1} is the template obtained from time $t - 1$, and μ is a constant regularization coefficient. We can interpret the three terms in the right-hand-side of the above equation as follows. The first term demands that the new template has to match the newly observed features accordingly with the assigned labels. The second term is the spatial regularization term which demands that regions outside of the box contribute less to the matching result. The third term corresponds to self-regularization that ensures smooth appearance change. To search for the box in frame $(t + 1)$, STRCF correlates template \mathbf{f}_t with the search region and determines the box by finding the location that gives the highest response. Although STRCF can model the appearance change for most sequences, it suffers from overfitting so that it is not able to adapt to largely deformable objects quickly. Furthermore, it cannot recover after

tracking loss.

The template model \mathbf{f} is updated at every frame with a fixed regularization coefficient μ in STRCF. In our implementation, we skip updating \mathbf{f} if no obvious motion is observed. In addition, a smaller μ is used when all modules agree with each other in prediction so that \mathbf{f} can quickly adapt to the new appearance for largely deformable objects.

Background motion modeling. For SOT, we can decompose the pixel displacement between adjacent frames (also called optical flow) into two types: object motion and background motion. Background motion is usually simpler so that it can be well modeled by a parametric model. Background motion estimation [37], [38] finds applications in video stabilization, coding and visual tracking. Here, we propose a 6-parameter model in form of

$$x_{t+1} = \alpha_1 x_t + \alpha_2 y_t + \alpha_0, \text{ and } y_{t+1} = \beta_1 x_t + \beta_2 y_t + \beta_0,$$

where (x_{t+1}, y_{t+1}) and (x_t, y_t) are corresponding background points in frames $(t + 1)$ and t , and α_i and β_i , $i = 0, 1, 2$ are model parameters. Given more than three pairs of corresponding points, we can solve the model parameters using the linear least-squares method. Usually, we choose a few salient points (e.g., corners) to build the correspondence and determine the parameters. We apply the background model to the grayscale image $I_t(x, y)$ of frame t to find the estimated $\hat{I}_{t+1}(x, y)$ of frame $(t + 1)$. Afterwards, we can compute the difference map ΔI :

$$\Delta I = \hat{I}_{t+1}(x, y) - I_{t+1}(x, y)$$

which is expected to have small and large values in the background and foreground regions, respectively. Thus, we can determine potential object locations. While the DCF-based baseline exploits foreground correlation to locate the object, background modeling uses background correlation to eliminate background influence in object tracking. They complement each other for some challenging task such as recovery from tracking loss. The DCF-based tracker cannot recover from tracking loss easily since it does not have a global view of the scene. In contrast, our background modeling module can still find potential locations of the object by removing the background region.

Trajectory-based Box Prediction. Given box centers of last N frames, $\{(x_{t-N}, y_{t-N}), \dots, (x_{t-1}, y_{t-1})\}$, we calculate $N - 1$ displacement vectors $\{(\Delta x_{t-N+1}, \Delta y_{t-N+1}), \dots, (\Delta x_{t-1}, \Delta y_{t-1})\}$ and apply the principal component analysis (PCA) to them. To predict

the displacement at frame t , we fit the first principal component using a line and set the second principal component to zero to remove noise. Then, the center location of the box at frame t can be written as

$$(\hat{x}_t, \hat{y}_t) = (x_{t-1}, y_{t-1}) + (\hat{\Delta}x_t, \hat{\Delta}y_t).$$

Similarly, we can estimate the width and the height of the box at frame t , denoted by (\hat{w}_t, \hat{h}_t) . Typically, the physical motion of an object has an inertia in motion trajectory and its size, and the box prediction process attempts to maintain the inertia. It contributes to better tracking performance in two ways. First, it can remove small fluctuation of the box in its location and size. Second, when there is a rapid deformation of the target object, the appearance model alone cannot capture the shape change effectively. In contrast, the combination of background motion modeling and the trajectory-based box prediction can offer a more satisfactory solution. An example is given in Fig. 3, which shows a frame of the *diving* sequence in the upper-left subfigure, where the green and the blue boxes are the ground truth and the result of UHP-SOT, respectively. Although a DCF-based tracker can detect the size change by comparing correlation scores at five image resolutions, it cannot estimate the change of its aspect ratio. In contrast, the residual image after background removal in UHP-SOT, as shown in the lower-left subfigure, reveals the object shape. We sum up the absolute pixel values of the residual image horizontally and vertically. We use a threshold to determine the two ends of an interval. Then, we have

$$\hat{w} = x_{\max} - x_{\min}, \text{ and } \hat{h} = y_{\max} - y_{\min}.$$

Note that the raw estimation may not be stable across different frames. Estimations that deviate too much from the trajectory of $(\Delta w_t, \Delta h_t)$ are rejected. Then, we have a robust yet flexibly deformable box proposal.

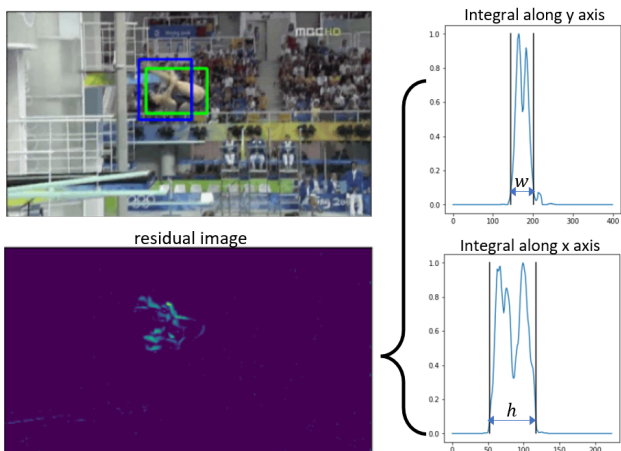


Fig. 3. Illustration of shape change estimation based on background motion model and the trajectory-based box prediction, where the ground truth and our proposal are in green and blue, respectively.

Fusion strategy. We have three box proposals for the target object at frame t : 1) B_{app} from the baseline tracker to capture appearance change, 2) B_{trj} from the trajectory predictor to maintain the inertia of box position/shape and 3) B_{bgd} from the background motion predictor to eliminate unlikely object regions. We need a fusion strategy to yield the final box location/shape, which is described below. We store two template models: the latest model \mathbf{f}_{t-1} , and an older model, \mathbf{f}_i , $i \leq t-1$, where i is the last time step where all three boxes have the same location. Model \mathbf{f}_i is less likely to be

contaminated since it needs agreement from all modules while B_{bgd} can jump around. To check the reliability of the three proposals, we compute correlation scores between three pairs: $(\mathbf{f}_{t-1}, B_{\text{app}})$, $(\mathbf{f}_{t-1}, B_{\text{trj}})$, and $(\mathbf{f}_i, B_{\text{bgd}})$ and then apply a rule-based fusion strategy:

- General rule: Choose the proposal with the highest score.
- Special rule: Although B_{app} has the highest score, we observe that B_{trj} has a close score, agrees with B_{bgd} , and reveals sudden jump (say, larger than 30 pixels). Then, we choose B_{trj} instead.

IV. EXPERIMENTS

Experimental Set-up. We compare UHP-SOT with state-of-the-art unsupervised and supervised trackers on TB-50 and TB-100 datasets [6]. The latter contains 100 videos and 59,040 frames. Evaluation is performed based on the ‘‘One Pass Evaluation (OPE)’’ protocol. Evaluation metrics include the precision plot (i.e., the distance of the predicted and actual box centers) and the success plot (i.e., overlapping ratios at various thresholds). The distance precision is measured at 20-pixel threshold to rank different methods. The overlap precision is measured by the area-under-curve (AUC) score. We use the same hyperparameter settings in STRCF except regularization coefficient μ . STRCF sets $\mu = 15$ while UHP-SOT selects $\mu \in \{10, 5, 0\}$ if the appearance box is not chosen. The smaller the correlation score, the smaller μ . We set $N = 20$ in the number of previous frames for trajectory prediction. The cutting threshold along horizontal/vertical directions is set to 0.1. UHP-SOT runs at 22.7 FPS on a PC equipped with an Intel(R) Core(TM) i5-9400F CPU, maintaining a near real-time speed (while STRCF operates at a speed of 24.3 FPS).

Performance Evaluation. Fig. 4 compares UHP-SOT with state-of-the-art unsupervised trackers ECO-HC [16], STRCF [12], SRDCFdecon [39], CSR-DCF [40], SRDCF [41], Staple [11], KCF [8], DSST [9] and supervised trackers SiamRPN++ [15], ECO [16], HDT [5], SiamFC_3s [29], LCT [42]. UHP-SOT outperforms STRCF by 4% in precision and 3.03% in overlap on TB-100 and 4% in precision and 2.7% in overlap on TB-50, respectively. As an unsupervised light-weight tracker, UHP-SOT achieves performance comparable with state-of-the-art deep trackers such as SiamRPN++ with ResNet-50 [43] as the backbone. UHP-SOT outperforms another deep tracker, ECO, which uses a Gaussian Mixture Model to store seen appearances and runs at around 10 FPS, in both accuracy and speed.

We show results on 10 challenging sequences on TB-100 for the top-4 trackers in Fig. 5. Generally, UHP-SOT can follow small moving objects or largely deformed objects like human body tightly even though some of them have occlusions. These are attributed to its quick recovery from tracking loss via background modeling and stability via trajectory prediction. On the other hand, UHP-SOT does not perform well for *Ironman* and *Matrix* because of rapid changes in both the foreground object and background. They exist in movie content due to editing in movie post-production. They do not occur in real-world object tracking. Deep trackers perform well for *Ironman* and *Matrix* by leveraging supervision.

We further analyze the performance variation under different challenging tracking scenarios for TB-100. We present the AUC score in Fig. 6 and compare with other state-of-the-art unsupervised DCF trackers STRCF, ECO-HC, and SRDCFdecon. Our method outperforms other trackers in all attributes, especially in deformation (DEF), in-plane rotation (IPR) and low resolution (LR). Difficult sequences in those attributes include *MotorRolling*, *Jump*, *Diving* and *Skiing*, where the target appearance changes fast due to large deformation. It is difficult to reach a high overlapping ratio without supervision or without an adaptive box aspect ratio strategy.

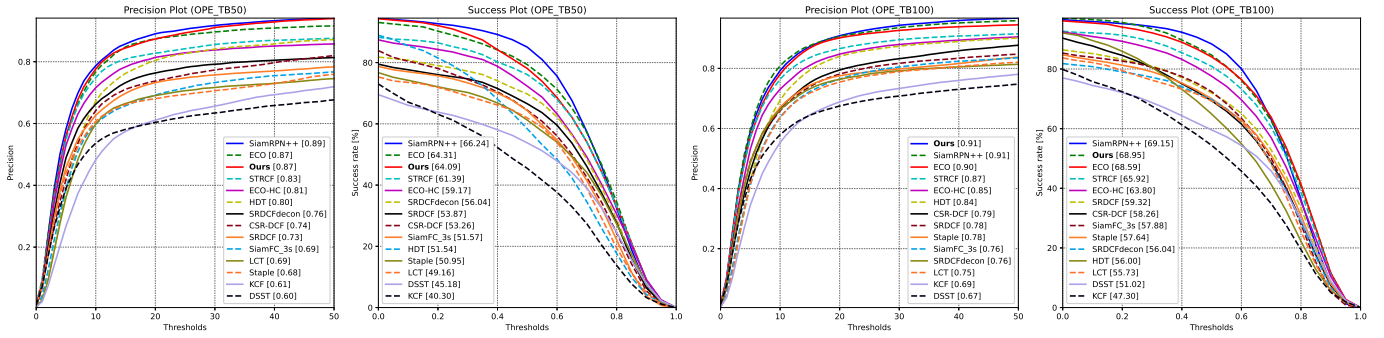


Fig. 4. The precision plot and the success plot on TB-50 and TB-100. To rank different methods, the distance precision is measured at 20-pixel threshold, and the overlap precision is measured by the AUC score. We collect other trackers’ raw results from the official websites to generate results.

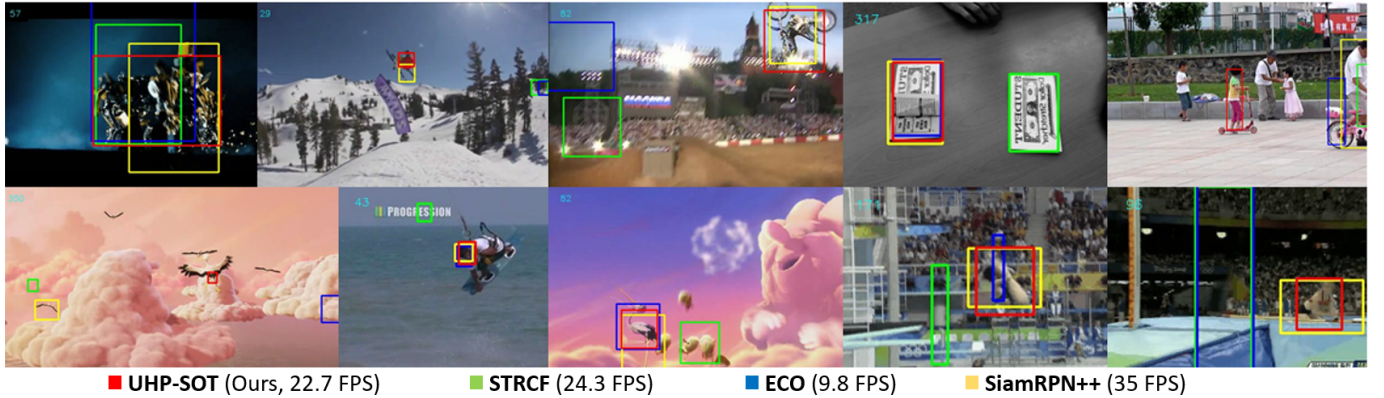


Fig. 5. Qualitative evaluation of UHP-SOT, STRCF [12], ECO [16] and SiamRPN++ [15] on 10 challenging videos from TB-100. They are (from left to right and top to down): *Trans*, *Skiing*, *MotorRolling*, *Coupon*, *Girl2*, *Bird1*, *KiteSurf*, *Bird2*, *Diving*, *Jump*, respectively.

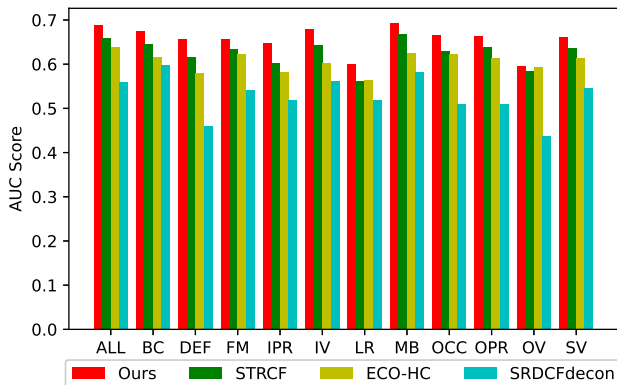


Fig. 6. Area-under-curve (AUC) score for attribute-based evaluation on the TB-100 dataset, where the 11 attributes are background clutter (BC), deformation (DEF), fast motion (FM), in-plane rotation (IPR), illumination variation (IV), low resolution (LR), motion blur (MB), occlusion (OCC), out-of-plane rotation (OPR), out-of-view (OV), and scale variation (SV), respectively.

Finally, we test two other variants of UHP-SOT: UHP-SOT-I (without trajectory prediction), and UHP-SOT-II (without background motion modeling) in Table I. The gap between UHP-SOT and UHP-SOT-I reveals the importance of inertia provided by trajectory prediction. UHP-SOT-I shows that background modeling does a good job in handling some difficult cases that STRCF cannot cope with,

leading to a gain of 2% in precision and 1.95% in overlap. UHP-SOT-II rejects large trajectory deviation and uses a smaller regularization coefficient to strengthen this correction. The accuracy of UHP-SOT-II drops more due to naive correction without confirmation from background modeling. Yet, it operates a much faster speed (32.02 FPS). Both background modeling and trajectory prediction are lightweight modules and run in real time.

TABLE I
PERFORMANCE OF UHP-SOT, UHP-SOT-I, UHP-SOT-II AND STRCF ON THE TB-100 DATASET, WHERE AUC IS USED FOR SUCCESS RATE.

	UHP-SOT	UHP-SOT-I	UHP-SOT-II	STRCF
Success (%)	68.95	67.87	65.64	65.92
Precision	0.91	0.89	0.87	0.87
Speed (FPS)	22.73	23.68	32.02	24.30

V. CONCLUSION AND FUTURE WORK

An unsupervised high-performance tracker called UHP-SOT, which uses STRCF as the baseline with two novel improvements, was proposed in this work. They are background motion modeling and a trajectory-based box prediction. It was shown by experimental results that UHP-SOT offers an effective real-time tracker in resource-limited platforms. Based on our study, object tracking appears to be a low-level vision problem where supervision may not be critical in all cases. To test this hypothesis we would like to apply supervised object detectors such as Yolo to edited movie sequences frame by frame and demonstrate the merit of supervision in the future.

REFERENCES

- [1] J. Xing, H. Ai, and S. Lao, "Multiple human tracking based on multi-view upper-body detection and discriminative learning," in *2010 20th International Conference on Pattern Recognition*. IEEE, 2010, pp. 1698–1701.
- [2] J. Janai, F. Güneý, A. Behl, A. Geiger *et al.*, "Computer vision for autonomous vehicles: Problems, datasets and state of the art," *Foundations and Trends® in Computer Graphics and Vision*, vol. 12, no. 1–3, pp. 1–308, 2020.
- [3] G. Zhang and P. A. Vela, "Good features to track for visual slam," in *Proceedings of the IEEE conference on computer vision and pattern recognition*, 2015, pp. 1373–1382.
- [4] A. Yilmaz, O. Javed, and M. Shah, "Object tracking: A survey," *Acm computing surveys (CSUR)*, vol. 38, no. 4, pp. 13–es, 2006.
- [5] M. Fiaz, A. Mahmood, S. Javed, and S. K. Jung, "Handcrafted and deep trackers: Recent visual object tracking approaches and trends," *ACM Computing Surveys (CSUR)*, vol. 52, no. 2, pp. 1–44, 2019.
- [6] Y. Wu, J. Lim, and M.-H. Yang, "Object tracking benchmark," *IEEE Transactions on Pattern Analysis and Machine Intelligence*, vol. 37, no. 9, pp. 1834–1848, 2015.
- [7] D. S. Bolme, J. R. Beveridge, B. A. Draper, and Y. M. Lui, "Visual object tracking using adaptive correlation filters," in *2010 IEEE computer society conference on computer vision and pattern recognition*. IEEE, 2010, pp. 2544–2550.
- [8] J. F. Henriques, R. Caseiro, P. Martins, and J. Batista, "High-speed tracking with kernelized correlation filters," *IEEE transactions on pattern analysis and machine intelligence*, vol. 37, no. 3, pp. 583–596, 2014.
- [9] M. Danelljan, G. Häger, F. S. Khan, and M. Felsberg, "Discriminative scale space tracking," *IEEE transactions on pattern analysis and machine intelligence*, vol. 39, no. 8, pp. 1561–1575, 2016.
- [10] M. Danelljan, A. Robinson, F. S. Khan, and M. Felsberg, "Beyond correlation filters: Learning continuous convolution operators for visual tracking," in *European conference on computer vision*. Springer, 2016, pp. 472–488.
- [11] L. Bertinetto, J. Valmadre, S. Golodetz, O. Miksik, and P. H. Torr, "Staple: Complementary learners for real-time tracking," in *Proceedings of the IEEE conference on computer vision and pattern recognition*, 2016, pp. 1401–1409.
- [12] F. Li, C. Tian, W. Zuo, L. Zhang, and M.-H. Yang, "Learning spatial-temporal regularized correlation filters for visual tracking," in *Proceedings of the IEEE conference on computer vision and pattern recognition*, 2018, pp. 4904–4913.
- [13] M. Danelljan, G. Hager, F. Shahbaz Khan, and M. Felsberg, "Convolutional features for correlation filter based visual tracking," in *Proceedings of the IEEE international conference on computer vision workshops*, 2015, pp. 58–66.
- [14] J. Valmadre, L. Bertinetto, J. Henriques, A. Vedaldi, and P. H. Torr, "End-to-end representation learning for correlation filter based tracking," in *Proceedings of the IEEE conference on computer vision and pattern recognition*, 2017, pp. 2805–2813.
- [15] B. Li, W. Wu, Q. Wang, F. Zhang, J. Xing, and J. Yan, "Siamrpn++: Evolution of siamese visual tracking with very deep networks," in *Proceedings of the IEEE/CVF Conference on Computer Vision and Pattern Recognition*, 2019, pp. 4282–4291.
- [16] M. Danelljan, G. Bhat, F. Shahbaz Khan, and M. Felsberg, "Eco: Efficient convolution operators for tracking," in *Proceedings of the IEEE conference on computer vision and pattern recognition*, 2017, pp. 6638–6646.
- [17] Z. Hong, Z. Chen, C. Wang, X. Mei, D. Prokhorov, and D. Tao, "Multi-store tracker (muster): A cognitive psychology inspired approach to object tracking," in *Proceedings of the IEEE conference on computer vision and pattern recognition*, 2015, pp. 749–758.
- [18] D. Held, S. Thrun, and S. Savarese, "Learning to track at 100 fps with deep regression networks," in *European conference on computer vision*. Springer, 2016, pp. 749–765.
- [19] A. Krizhevsky, I. Sutskever, and G. E. Hinton, "Imagenet classification with deep convolutional neural networks," *Advances in neural information processing systems*, vol. 25, pp. 1097–1105, 2012.
- [20] K. Chatfield, K. Simonyan, A. Vedaldi, and A. Zisserman, "Return of the devil in the details: Delving deep into convolutional nets," *arXiv preprint arXiv:1405.3531*, 2014.
- [21] C. Ma, J.-B. Huang, X. Yang, and M.-H. Yang, "Hierarchical convolutional features for visual tracking," in *Proceedings of the IEEE international conference on computer vision*, 2015, pp. 3074–3082.
- [22] Y. Qi, S. Zhang, L. Qin, H. Yao, Q. Huang, J. Lim, and M.-H. Yang, "Hedged deep tracking," in *Proceedings of the IEEE conference on computer vision and pattern recognition*, 2016, pp. 4303–4311.
- [23] N. Wang, W. Zhou, Q. Tian, R. Hong, M. Wang, and H. Li, "Multicue correlation filters for robust visual tracking," in *Proceedings of the IEEE conference on computer vision and pattern recognition*, 2018, pp. 4844–4853.
- [24] B. Li, J. Yan, W. Wu, Z. Zhu, and X. Hu, "High performance visual tracking with siamese region proposal network," in *Proceedings of the IEEE conference on computer vision and pattern recognition*, 2018, pp. 8971–8980.
- [25] X. Lu, C. Ma, B. Ni, X. Yang, I. Reid, and M.-H. Yang, "Deep regression tracking with shrinkage loss," in *Proceedings of the European conference on computer vision (ECCV)*, 2018, pp. 353–369.
- [26] H. Nam and B. Han, "Learning multi-domain convolutional neural networks for visual tracking," in *Proceedings of the IEEE conference on computer vision and pattern recognition*, 2016, pp. 4293–4302.
- [27] S. Pu, Y. Song, C. Ma, H. Zhang, and M.-H. Yang, "Deep attentive tracking via reciprocative learning," *arXiv preprint arXiv:1810.03851*, 2018.
- [28] Y. Song, C. Ma, L. Gong, J. Zhang, R. W. Lau, and M.-H. Yang, "Crest: Convolutional residual learning for visual tracking," in *Proceedings of the IEEE international conference on computer vision*, 2017, pp. 2555–2564.
- [29] L. Bertinetto, J. Valmadre, J. F. Henriques, A. Vedaldi, and P. H. Torr, "Fully-convolutional siamese networks for object tracking," in *European conference on computer vision*. Springer, 2016, pp. 850–865.
- [30] R. Tao, E. Gavves, and A. W. Smeulders, "Siamese instance search for tracking," in *Proceedings of the IEEE conference on computer vision and pattern recognition*, 2016, pp. 1420–1429.
- [31] Z. Zhu, Q. Wang, B. Li, W. Wu, J. Yan, and W. Hu, "Distractor-aware siamese networks for visual object tracking," in *Proceedings of the European Conference on Computer Vision (ECCV)*, 2018, pp. 101–117.
- [32] Q. Wang, Z. Teng, J. Xing, J. Gao, W. Hu, and S. Maybank, "Learning attentions: residual attentional siamese network for high performance online visual tracking," in *Proceedings of the IEEE conference on computer vision and pattern recognition*, 2018, pp. 4854–4863.
- [33] A. He, C. Luo, X. Tian, and W. Zeng, "A twofold siamese network for real-time object tracking," in *Proceedings of the IEEE Conference on Computer Vision and Pattern Recognition*, 2018, pp. 4834–4843.
- [34] N. Wang and D. Y. Yeung, "Learning a deep compact image representation for visual tracking," *Advances in neural information processing systems*, 2013.
- [35] N. Wang, Y. Song, C. Ma, W. Zhou, W. Liu, and H. Li, "Unsupervised deep tracking," in *Proceedings of the IEEE/CVF Conference on Computer Vision and Pattern Recognition*, 2019, pp. 1308–1317.
- [36] M. Danelljan, F. Shahbaz Khan, M. Felsberg, and J. Van de Weijer, "Adaptive color attributes for real-time visual tracking," in *Proceedings of the IEEE Conference on Computer Vision and Pattern Recognition*, 2014, pp. 1090–1097.
- [37] K. Hariharakrishnan and D. Schonfeld, "Fast object tracking using adaptive block matching," *IEEE transactions on multimedia*, vol. 7, no. 5, pp. 853–859, 2005.
- [38] A. Aggarwal, S. Biswas, S. Singh, S. Sural, and A. K. Majumdar, "Object tracking using background subtraction and motion estimation in mpeg videos," in *Asian Conference on Computer Vision*. Springer, 2006, pp. 121–130.
- [39] M. Danelljan, G. Hager, F. Shahbaz Khan, and M. Felsberg, "Adaptive decontamination of the training set: A unified formulation for discriminative visual tracking," in *Proceedings of the IEEE Conference on Computer Vision and Pattern Recognition*, 2016, pp. 1430–1438.
- [40] L. Alan, T. Vojř, L. Čehovin, J. Matas, and M. Kristan, "Discriminative correlation filter tracker with channel and spatial reliability," *International Journal of Computer Vision*, vol. 126, no. 7, pp. 671–688, 2018.
- [41] M. Danelljan, G. Hager, F. Shahbaz Khan, and M. Felsberg, "Learning spatially regularized correlation filters for visual tracking," in *Proceedings of the IEEE international conference on computer vision*, 2015, pp. 4310–4318.
- [42] C. Ma, X. Yang, C. Zhang, and M.-H. Yang, "Long-term correlation tracking," in *Proceedings of the IEEE conference on computer vision and pattern recognition*, 2015, pp. 5388–5396.
- [43] K. He, X. Zhang, S. Ren, and J. Sun, "Deep residual learning for image recognition," in *Proceedings of the IEEE conference on computer vision and pattern recognition*, 2016, pp. 770–778.